arXiv:1105.1110v1 [hep-ph] 5 May 2011

# SQUARK AND GLUINO HADROPRODUCTION

WIM BEENAKKER
*Theoretical High Energy Physics, IMAPP, Radboud University Nijmegen, P.O. Box 9010*
*NL-6500 GL Nijmegen, The Netherlands*
*W.Beenakker@science.ru.nl*

SILJA BRENSING
*DESY, Theory Group Notkestrasse 85, D-22603 Hamburg, Germany*
*silja.christine.brensing@desy.de*

MICHAEL KRÄMER
*Institute for Theoretical Particle Physics and Cosmology, RWTH Aachen University*
*D-52056 Aachen, Germany*
*mkraemer@physik.rwth-aachen.de*

ANNA KULESZA
*Institute for Theoretical Particle Physics and Cosmology, RWTH Aachen University*
*D-52056 Aachen, Germany*
*anna.kulesza@physik.rwth-aachen.de*

ERIC LAENEN
*ITFA, University of Amsterdam, Science Park 904, 1090 GL Amsterdam,*
*ITF, Utrecht University, Leuvenlaan 4, 3584 CE Utrecht*
*Nikhef, Science Park 105, 1098 XG Amsterdam, The Netherlands*
*Eric.Laenen@nikhef.nl*

LESZEK MOTYKA
*Institute of Physics, Jagellonian University, Reymonta 4, 30-059 Kraków, Poland*
*leszekm@th.if.uj.edu.pl*

IRENE NIESSEN
*Theoretical High Energy Physics, IMAPP, Radboud University Nijmegen, P.O. Box 9010*
*NL-6500 GL Nijmegen, The Netherlands*
*i.niessen@science.ru.nl*

We review the theoretical status of squark and gluino hadroproduction and provide numerical predictions for all squark and gluino pair-production processes at the Tevatron and at the LHC, with a particular emphasis on proton-proton collisions at 7 TeV. Our predictions include next-to-leading order supersymmetric QCD corrections and the resummation of soft gluon emission at next-to-leading-logarithmic accuracy. We discuss the impact of the higher-order corrections on total cross sections, and provide an estimate of the theoretical uncertainty due to scale variation and the parton distribution functions.

*Keywords*: Supersymmetry; QCD; resummation.

PACS numbers: 11.25.Hf, 123.1K

Preprint numbers: DESY 11-060, ITFA 11-09, ITP-UU-11/13, Nikhef-2011-011, TTK 11-12

## 1. Introduction

The search for supersymmetry (SUSY)[1,2] is a central part of the experimental program at the hadron colliders Tevatron and LHC. Models of weak-scale SUSY provide a promising solution to the hierarchy problem of the Standard Model (SM) and comprise new supersymmetric particles (sparticles) with masses of order 1 TeV. The coloured TeV-scale sparticles, squarks ($\tilde{q}$) and gluinos ($\tilde{g}$), would be produced copiously in hadronic collisions and thus offer the strongest sensitivity for supersymmetry searches at the Tevatron and the LHC.

We consider the minimal supersymmetric extension of the Standard Model (MSSM)[3,4] where, as a consequence of R-parity conservation, squarks and gluinos are pair-produced in collisions of two hadrons $h_1$ and $h_2$:

$$h_1 h_2 \;\rightarrow\; \tilde{q}\tilde{q}\,, \tilde{q}\bar{\tilde{q}}\,, \tilde{q}\tilde{g}\,, \tilde{g}\tilde{g},\, \tilde{t}_1\bar{\tilde{t}}_1,\, \tilde{t}_2\bar{\tilde{t}}_2 + X\,. \tag{1}$$

The production of top squarks (stops), $\tilde{t}_{1,2}$, has to be treated separately, because the strong Yukawa coupling between top quarks, stops and Higgs fields gives rise to potentially large mixing effects and mass splitting.[5] In Eq. (1) and throughout the rest of this paper, $\tilde{t}_1$ and $\tilde{t}_2$ denote the lighter and heavier stop mass eigenstate, respectively. For the other squarks we suppress the chiralities, i.e. $\tilde{q} = (\tilde{q}_L, \tilde{q}_R)$, and do not explicitly state the charge-conjugated processes.

Searches for squarks and gluinos at the proton–antiproton collider Tevatron with a centre-of-mass energy of $\sqrt{S} = 1.96$ TeV have placed lower limits on squark and gluino masses in the range of 300 to 400 GeV, depending in detail on the specific SUSY model.[6,7] The proton–proton collider LHC, which has been operating at $\sqrt{S} = 7$ TeV in 2010, has already significantly extended the squark and gluino mass limits to values of around 850 GeV.[8–13] Dedicated searches for the lighter stop mass eigenstate at LEP[14,15] and the Tevatron[16–18] have placed lower limits in the range 70 to 200 GeV. Already in 2011, with a projected integrated luminosity of 1 to 2 $\text{fb}^{-1}$, the LHC should be sensitive to squarks and gluinos with masses in the TeV region[19], while SUSY particles with masses up to 3 TeV can be probed once the LHC reaches its design energy of $\sqrt{S} = 14$ TeV.[20,21]

Accurate theoretical predictions for inclusive squark and gluino cross sections are needed both to set exclusion limits and, in case SUSY is discovered, to determine SUSY particle masses and properties.[22–25] The inclusion of higher-order SUSY-QCD corrections significantly reduces the renormalization- and factorization-scale dependence of the predictions. In general, the corrections also increase the size of the cross section with respect to the leading-order prediction[26–28] if the renormalization and factorization scales are chosen close to the average mass of the produced SUSY particles. Consequently, the SUSY-QCD corrections have a substantial impact on the determination of mass exclusion limits and would lead to a significant reduction of errors on SUSY mass or parameter values in the case of discovery. The processes listed in Eq. (1) have been known for quite some time at next-to-leading order (NLO) in SUSY-QCD.[29–32] Electroweak corrections to the $\mathcal{O}(\alpha_s^2)$ tree-level processes[33–39] and the electroweak Born production channels of $\mathcal{O}(\alpha\alpha_s)$ and $\mathcal{O}(\alpha^2)$[40,41] are in general significant for the pair production of SU(2)-doublet squarks $\tilde{q}_L$ and at large invariant masses, but they are moderate for inclusive cross sections.

A significant part of the NLO QCD corrections can be attributed to the threshold region, where the partonic centre-of-mass energy is close to the kinematic production threshold. In this region the NLO corrections are dominated by soft gluon emission off the coloured particles in the initial and final state and by the Coulomb corrections due to the exchange of gluons between the massive sparticles in the final state. The soft-gluon corrections can be taken into account to all orders in perturbation theory by means of threshold resummation techniques.[42,43]

Recently, such a threshold resummation has been performed for all MSSM squark and gluino production processes, Eq. (1), at next-to-leading-logarithmic (NLL) accuracy.[44–47] A formalism has been developed in the framework of effective field theories which allows for the resummation of soft and Coulomb gluons in the production of coloured sparticles, but has so far only been applied to squark-antisquark production.[48,49] In addition, the dominant next-to-next-to-leading order (NNLO) corrections, including those coming from the resummed cross section at next-to-next-to-leading-logarithmic (NNLL) level, have been calculated for squark-antisquark pair-production.[50,51] The production of gluino bound states as well as bound-state effects in gluino-pair production has also been studied.[52,53]

In this work we will present the state-of-the-art SUSY-QCD predictions for the MSSM squark and gluino hadroproduction processes, Eq. (1), at the Tevatron and the LHC, including NLO corrections and NLL threshold resummation. The processes will all be treated on the same footing, i.e. classes of beyond-NLO effects that have been calculated only for one particular process or reaction channel will not be taken into account. We will discuss the impact of the SUSY-QCD corrections on the total cross sections and provide an estimate of the theoretical uncertainty due to scale variation, parton distribution functions, and the strong coupling $\alpha_s$.

The structure of the paper is as follows. In section 2 we briefly review the application of the resummation technique to total cross sections for coloured sparticle pair-production. The numerical results are presented in section 3. We show predictions for the Tevatron, and for the LHC with centre-of-mass energies of $\sqrt{S} = 7$ TeV and $\sqrt{S} = 14$ TeV. We will conclude in section 4.

## 2. NLL resummation

In this section we provide a brief background to the calculation of the threshold-resummed cross sections[44–46] we use for our results in the next section. The resummation for 2 → 2 processes with all four external legs carrying colour has been studied extensively in the literature, specifically for heavy-quark[54,55] and jet production.[56–58] In our calculations we make use of the framework developed there.

The hadronic threshold for the inclusive production of two final-state particles $k, l$ with masses $m_k$ and $m_l$ corresponds to a hadronic centre-of-mass energy squared that is equal to $S = (m_k + m_l)^2$. Thus we define the threshold variable $\rho$, measuring the distance from threshold in terms of energy fraction, as

$$\rho \;=\; \frac{(m_k + m_l)^2}{S}\,. \tag{2}$$

Our results are based on the following expression for the NLL-resummed cross section, matched to the exact NLO calculation[29–32]

$$\begin{aligned}\sigma^{(\text{NLO+NLL})}_{h_1 h_2 \to kl}\big(\rho, \{m^2\}, \mu^2\big) &= \sigma^{(\text{NLO})}_{h_1 h_2 \to kl}\big(\rho, \{m^2\}, \mu^2\big) \\ &+ \frac{1}{2\pi i} \sum_{i,j=q,\bar{q},g} \int_{\text{CT}} dN\, \rho^{-N}\, \tilde{f}_{i/h_1}(N+1, \mu^2)\, \tilde{f}_{j/h_2}(N+1, \mu^2) \\ &\times \Big[\tilde{\sigma}^{(\text{res})}_{ij \to kl}\big(N, \{m^2\}, \mu^2\big) \;-\; \tilde{\sigma}^{(\text{res})}_{ij \to kl}\big(N, \{m^2\}, \mu^2\big)\,|_{(\text{NLO})}\Big]\,,\end{aligned} \tag{3}$$

where the last term in the square brackets denotes the NLL resummed expression expanded to NLO. The initial state hadrons are denoted generically as $h_1$ and $h_2$, and $\mu$ is the common factorization and renormalization scale. The resummation is performed after taking a Mellin transform (indicated by a tilde) of the cross section,

$$\tilde{\sigma}_{h_1 h_2 \to kl}\big(N, \{m^2\}\big) \equiv \int_0^1 d\rho\, \rho^{N-1}\, \sigma_{h_1 h_2 \to kl}\big(\rho, \{m^2\}\big)\,. \tag{4}$$

To evaluate the contour CT of the inverse Mellin transform in Eq. (3) we adopt the so-called "minimal prescription".[59] The NLL resummed cross section in Eq. (3) reads

$$\begin{aligned}\tilde{\sigma}^{(\text{res})}_{ij \to kl}\big(N, \{m^2\}, \mu^2\big) &= \sum_I \tilde{\sigma}^{(0)}_{ij \to kl, I}\big(N, \{m^2\}, \mu^2\big)\, C_{ij \to kl, I}\big(N, \{m^2\}, \mu^2\big) \\ &\times \Delta_i(N+1, Q^2, \mu^2)\, \Delta_j(N+1, Q^2, \mu^2)\, \Delta^{(\text{s})}_{ij \to kl, I}\big(N+1, Q^2, \mu^2\big)\,,\end{aligned} \tag{5}$$

where $\tilde{\sigma}^{(0)}_{ij \to kl, I}$ are the colour-decomposed leading-order cross sections in Mellin-moment space, with $I$ labelling the possible colour structures.[45,46] Here we have introduced the hard scale $Q^2 = (m_k + m_l)^2$. The perturbative functions $C_{ij \to kl, I}$ contain information about hard contributions beyond leading order. This information is only relevant beyond NLL accuracy and therefore we keep $C_{ij \to kl, I} = 1$ in our calculations. The functions $\Delta_i$ and $\Delta_j$ sum the effects of the (soft-)collinear radiation from the incoming partons. They are process-independent and do not depend on the colour structures. They contain the leading logarithmic dependence, as well as part of the subleading logarithmic behaviour. The expressions for $\Delta_i$ and $\Delta_j$ can be found in the literature.[45] The resummation of the soft-gluon contributions, which does depend on the colour structures in which the final state SUSY particle pairs can be produced, contributes at the NLL level and is summarized by the factor

$$\Delta_I^{(\mathrm{s})}\big(N, Q^2, \mu^2\big) \;=\; \exp\left[\int_{\mu}^{Q/N} \frac{dq}{q}\,\frac{\alpha_{\mathrm{s}}(q)}{\pi}\,D_I\right]. \tag{6}$$

The one-loop coefficients $D_I$ follow from the threshold limit of the one-loop soft anomalous-dimension matrix.[45,46]

Two remarks can be made regarding squark-gluino production, and stop-antistop production in particular. The former reaction is the only one in our set where heavy, coloured SUSY particles of different mass are produced. Our resummed expressions are sensitive to these differences through the Born cross sections, and through the resummed exponents at the NLL level.[46] In stop-antistop production through $q\bar{q}$ annihilation the gluino exchange diagram, which would require top parton distribution functions, is missing in the five-flavour scheme we adopt. As a consequence, the Born cross section for stop production is proportional to $\left(\sqrt{1-4m_{\tilde{q}}^2/s}\right)^3$, as opposed to $\sqrt{1-4m_{\tilde{q}}^2/s}$ for production of the other squark flavours. Here, $m_{\tilde{q}}$ is a generic squark mass and $s$ denotes the partonic centre-of-mass energy squared. We have argued[47] that this has no effect on the resummed expression other than through the explicit expression for the Born function.

## 3. Numerical Results

We present numerical predictions for squark and gluino production at the Tevatron ($\sqrt{S} = 1.96$ TeV) and the LHC ($\sqrt{S} = 7$ and 14 TeV). We compare LO, NLO and NLO+NLL matched results, and discuss the theoretical uncertainty due to the choice of renormalization and factorization scales and due to the uncertainty in the parton distribution functions (pdfs) and the QCD coupling $\alpha_{\mathrm{s}}$. The LO and NLO cross sections[29–32] are available in the form of the public computer code `Prospino`.[60] The $\overline{\mathrm{MS}}$-scheme with five active flavours is used to define $\alpha_{\mathrm{s}}$ and the parton distribution functions at NLO. The masses of the squarks and gluinos are renormalized in the on-shell scheme, and the SUSY particles are decoupled from the running of $\alpha_{\mathrm{s}}$ and the pdfs.

As mentioned in the introduction, the production of stops has to be treated separately because of potentially large mixing effects and mass splitting. The production of the other squark flavours, which we assume to be mass degenerate, is treated together, i.e. we sum over five flavours of squarks, $\tilde{q} \in \{\tilde{u}, \tilde{d}, \tilde{c}, \tilde{s}, \tilde{b}\}$. In that case our numerical predictions include both chiralities ($\tilde{q}_L$ and $\tilde{q}_R$) and the charge-conjugated processes.

The stop cross section is shown separately. Note that since mixing in the stop sector enters explicitly only through higher-order diagrams, the stop-mixing angle

$\theta_{\tilde{t}}$ need not be renormalized and one can use the lowest-order expression derived from the stop mass matrix. Beyond LO the stop cross section does not only depend on the stop mass, but also on the gluino mass $m_{\tilde{g}}$, the average mass of the first and second generation squarks $m_{\tilde{q}}$ and the mixing angle $\theta_{\tilde{t}}$. We have fixed $m_{\tilde{g}}$, $m_{\tilde{q}}$ and $\theta_{\tilde{t}}$ according to the SPS1a' benchmark scenario.[61] Note, however, that the dependence of the stop cross section on the SUSY parameters that enter only at NLO is numerically very small with variations of at most 2%.[47] The numerical results presented for stop production also apply to sbottom production when the same input parameters are adopted, since the impact of bottom-quark induced contributions to sbottom hadroproduction is negligible.[47]

For convenience we define the average mass of the final-state sparticle pair $m = (m_k + m_l)/2$, which reduces to the squark and gluino mass for $\tilde{q}\bar{\tilde{q}}$, $\tilde{q}\tilde{q}$, and $\tilde{g}\tilde{g}$ final states, respectively. The renormalization and factorization scales are taken to be equal, $\mu_{\mathrm{R}} = \mu_{\mathrm{F}} = \mu$. As our default, hadronic NLO and NLO+NLL cross sections are obtained with the 2008 NLO MSTW pdfs[62] and the corresponding $\alpha_{\mathrm{s}}(M_Z) = 0.120$. In particular, all plots show results for the MSTW pdf set.[62] We also present results based on the CT10[64] and CTEQ6L1[65] pdf sets in tables, for comparison.

Let us now discuss the numerical results for squark and gluino hadroproduction at the Tevatron, and at the LHC operating with 7 and 14 TeV hadronic centre-of-mass energy. We shall study the scale dependence of the LO, NLO and NLO+NLL cross sections, the impact of the NLL threshold resummation, and present our best predictions at NLO+NLL for the inclusive cross sections, including the theoretical uncertainties from scale variation as well as the pdf and $\alpha_{\mathrm{s}}$ errors. We put special emphasis on the predictions for the LHC at 7 TeV energy, which are of immediate importance for the upcoming SUSY searches, and collect detailed results for representative LO, NLO and NLO+NLL cross sections and the corresponding theory uncertainties in tables.

### 3.1. *Tevatron*

The state-of-the-art NLO+NLL SUSY-QCD cross-section predictions for the individual processes listed in Eq. (1), occuring in $p\bar{p}$ collisions at the Tevatron, are shown in Fig. 1 as a function of the average mass $m$ of the final state sparticles. For illustration we show these results for the case $m_{\tilde{q}} = m_{\tilde{g}}$. In Fig. 2 the total NLO+NLL cross section for the sum of all four processes, i.e. $\tilde{q}\tilde{q}$ , $\tilde{q}\bar{\tilde{q}}$ , $\tilde{q}\tilde{g}$ and $\tilde{g}\tilde{g}$ production, is presented. For the central values, the renormalization and factorization scales are taken as $\mu = \mu_0 = m$, which is the scale choice adopted as the preferred one in the context of the NLO SUSY-QCD calculations.[29–32] The error band represents an estimate of the theoretical uncertainty of the cross section prediction. It consists of the 68% C.L. pdf and $\alpha_{\mathrm{s}}$ error, added in quadrature, and the error from scale variation in the range $m/2 \leq \mu \leq 2m$ added linearly to the combined pdf and $\alpha_{\mathrm{s}}$ uncertainty. By this linear combination of scale uncertainty and combined pdf and

$\alpha_{\rm s}$ errors we provide a conservative estimate of the theory error.

At the scale $\mu = m$ the cross-section predictions are enhanced by soft-gluon resummation. The relative $K$-factor $K_{\rm NLL} = \sigma_{\rm NLO+NLL}/\sigma_{\rm NLO}$ for this scale choice is displayed in Fig. 3 for squark and gluino masses in the range between 200 and 600 GeV, and stop masses between 100 and 300 GeV. The soft-gluon corrections are moderate for $\tilde{q}\bar{\tilde{q}}$ and $\tilde{t}_1\bar{\tilde{t}}_1$ production, but increase the predictions for $\tilde{q}\tilde{q}$, $\tilde{g}\tilde{g}$ and $\tilde{q}\tilde{g}$ final states by around 15, 20 and 40%, respectively, assuming squark and gluino masses near 500 GeV. Because of the increasing importance of the threshold region, the corrections in general become larger for increasing sparticle masses. The large effect of soft-gluon resummation for $\tilde{q}\tilde{g}$ and $\tilde{g}\tilde{g}$ production can be mostly attributed to the importance of gluon initial states for these processes. Furthermore, the presence of gluinos in the final state results in an enhancement of the NLL contributions, since in this case the Casimir invariants that enter the $D_I$ coefficients in Eq. (6) are larger than for processes involving only squarks. The substantial value of $K_{\rm NLL}$ for $\tilde{q}\tilde{q}$ production at the Tevatron is a consequence of the behaviour of the corresponding NLO corrections[31], which strongly decrease with increasing squark mass.

Let us next discuss the scale dependence of the SUSY-QCD cross-section prediction in some more detail. Fig. 4 shows the scale dependence in LO, NLO and NLO+NLL for the different production processes, listed in Eq. (1), at the Tevatron. The mass of the $(\tilde{u}, \tilde{d}, \tilde{c}, \tilde{s}, \tilde{b})$-squarks and the gluino mass have been set to $m_{\tilde{q}} = m_{\tilde{g}} = 500\,\text{GeV}$, while the stop mass is fixed to $m_{\tilde{t}_1} = 200\,\text{GeV}$. Note that the LO predictions are obtained with the LO MSTW pdf set[62] and the corresponding LO value for $\alpha_{\rm s}$. The renormalization and factorization scales are set equal to each other and varied around the average mass of the final state sparticles, $\mu_0 = m$. We observe the usual strong reduction of the scale dependence when going from LO to NLO. A further significant improvement is obtained when the resummation of threshold logarithms is included, in particular for $\tilde{g}\tilde{g}$ and $\tilde{q}\tilde{g}$ production. For the $\tilde{q}\bar{\tilde{q}}$, $\tilde{q}\tilde{g}$ and $\tilde{g}\tilde{g}$ final states, contributing the most to the inclusive squark and gluino cross section at the Tevatron, the LO, NLO and NLO+NLL cross section predictions converge particularly well near $\mu = m/2$, which appears to be the preferred scale choice for these processes.

### 3.2. *LHC @ 7 TeV*

SUSY searches at the LHC, which is currently operating at 7 TeV, will soon be sensitive to sparticles with masses in the TeV-range. We thus discuss the cross section predictions for the LHC @ 7 TeV in more detail, including in particular the dependence of the NLL corrections on the ratio of the gluino and squark masses, and the size of the theory uncertainty due to scale, pdf and $\alpha_{\rm s}$ errors.

As before, we first present the NLO+NLL cross section predictions for the five individual processes and for the sum of the $\tilde{q}\tilde{q}$, $\tilde{q}\bar{\tilde{q}}$, $\tilde{q}\tilde{g}$, $\tilde{g}\tilde{g}$ final states, cf. Figs. 5 and 6. We include the estimate of the theory uncertainty obtained from adding linearly the scale dependence in the range $m/2 \leq \mu \leq 2m$ to the combined 68% C.L. pdf and $\alpha_{\rm s}$ error, added in quadrature.

In Fig. 7 we show the enhancement of the cross section due to the NLL resummation at the scale $\mu = m$. For gluino-pair and squark-gluino production processes we find a significant increase of 10-20% at masses around 1 TeV. An enhancement of up to 10% can also be observed for the production of heavy stop particles. Note that the singularities at the stop-decay threshold $m_{\tilde{t}} = m_t + m_{\tilde{g}} = 782.5\,\text{GeV}$ originate from the stop wave-function renormalization. They are an unphysical artefact of an on-shell scheme approach[32] and could be removed by taking into account the finite widths of the unstable stops. The effect of the NLL resummation on the cross section for inclusive squark and gluino production is shown in Fig. 8.

Next, we present the scale dependence in LO, NLO and NLO+NLL for the various production processes, see Fig. 9. Here, the mass of the $(\tilde{u}, \tilde{d}, \tilde{c}, \tilde{s}, \tilde{b})$-squarks and the gluino mass have been set to $m_{\tilde{q}} = m_{\tilde{g}} = 700\,\text{GeV}$, while the stop mass is fixed to $m_{\tilde{t}_1} = 500\,\text{GeV}$. As anticipated, we observe a significant reduction of the scale dependence when going from LO to NLO and from NLO to NLO+NLL. Note that also for squark and gluino production at the LHC, the convergence of the LO, NLO and NLO+NLL cross section predictions near the scale $\mu = m/2$ is striking.

As the cross section predictions for the LHC operating at 7 TeV are of particular phenomenological importance, let us discuss the results in some more detail. First, we collect representative values for LO, NLO and NLO+NLL cross sections in Tables 1-3. We include the scale dependence in the range $m/2 \leq \mu \leq 2m$ for the LO, NLO and NLO+NLL calculations, and the 68% C.L. pdf [a] and $\alpha_{\rm s}$ error at NLO. The NLO and NLL $K$-factors are displayed for convenience. The NLO and NLO+NLL theory predictions with the default MSTW pdf set[62] are compared to those obtained with the CT10 pdf set[64]. The LO cross sections are calculated with the LO MSTW[62] and the CTEQ6L1[65] pdfs. While the LO cross sections differ significantly between the two pdf sets, the central NLO+NLL predictions are consistent within the theoretical uncertainty. Note, however, that the 68% C.L. pdf error estimate for the CT10 set, obtained through rescaling of the 90% CL error estimate[66], is significantly larger than that of MSTW.

The size of the cross section and the impact of the higher-order corrections depends on the ratio $r = m_{\tilde{g}}/m_{\tilde{q}}$. In Fig. 10 we thus present the NLL $K$-factor for different values of $r$ for individual processes with the $\tilde{q}\tilde{q}$ , $\tilde{q}\bar{\tilde{q}}$ , $\tilde{q}\tilde{g}$ , $\tilde{g}\tilde{g}$ final states . In general, in the range of values of $r$ studied here, the dependence of the soft-gluon enhancement on $r$ is moderate. Of particular interest is the limit $r \to 0$, i.e. the limit of very heavy squarks. Such scenarios are predicted within so-called models of split supersymmetry[67] and lead to interesting new phenomenological signatures at the LHC, like long-lived gluinos.[68,69] In Fig. 11 we present the NLO+NLL cross section prediction for gluino-pair production in the limit $r = 0$ and show the impact of soft-gluon resummation. The $\tilde{g}\tilde{g}$ cross section for $r = 0$ is higher than for $r = 1$, with the difference growing from a factor of 1.2 at $m = 200$ GeV up to a factor of 4.7 for $m = 1.2$ TeV. The impact of soft-gluon resummation is significant, and the NLL corrections enhance the cross section by about 12% for gluinos with masses around 1 TeV.

---

[a] The pdf errors presented in the tables apply to individual processes only. In general, the pdf error for inclusive squark and gluino production will differ from the one obtained through combination of errors for individual processes due to possible correlations between various production channels.

The enhancement of the cross section prediction due to higher-order corrections depends, of course, on the choice of scale. Choosing $\mu = m/2$, we find in general NLL $K$-factors close to one for sparticle cross sections at the LHC with 7 TeV. However, a crucial improvement when going from LO to NLO and from NLO to NLO+NLL is the reduction of the scale dependence. Fig. 12 shows a comparison of the NLO and the NLO+NLL scale dependence for the sum of the $\tilde{q}\tilde{q}\,, \tilde{q}\bar{\tilde{q}}\,, \tilde{q}\tilde{g}\,, \tilde{g}\tilde{g}$ final states as a function of the average sparticle mass, assuming $r = 1$. Threshold resummation leads to a significant reduction of the scale dependence over the full range of sparticle masses, with an overall scale uncertainty at NLO+NLL of less than 10%. In a phenomenological analysis, the different production channels may contribute with different weight, depending in detail on the signature and the choice of selection cuts. Thus, we plot the scale uncertainty at NLO+NLL for the different channels in Fig. 13. We also show the full theory uncertainty, consisting of the 68% C.L. pdf and $\alpha_{\rm s}$ error added in quadrature, combined linearly with the scale variation error for the NLO cross sections and for the NLO+NLL cross sections. We find that even though the pdf uncertainty is significant, the inclusion of threshold resummation leads to a sizeable reduction of the overall theory uncertainty. This is particularly true for the case of gluino-pair and squark-gluino production. For gluino-pair production, the total theory uncertainty can be reduced by as much as a factor of two when going from NLO to NLO+NLL. Looking at all different production processes, the overall theory uncertainty at NLO+NLL is approximately 20% or smaller.

### 3.3. *LHC @ 14 TeV*

SUSY particles with masses in the multi-TeV region can be probed at the LHC running at or near its design energy of 14 TeV.[20,21] To complete this review and to show how the impact of the higher-order corrections depends on the collider energy, we also present predictions for squark and gluino production at the LHC with 14 TeV. Our cross section predictions at NLO+NLL including the full theory uncertainty, consisting of the 68% C.L. pdf and $\alpha_{\rm s}$ error, added in quadrature, combined linearly with the scale variation error, are shown in Figs. 14 and 15. As for the LHC at 7 TeV, the impact of NLL threshold resummation is particularly significant for gluino-pair and squark-gluino production, with NLL corrections of about 30% for $\tilde{g}\tilde{g}$ final states and squark and gluino masses of 2.5 TeV, see Fig. 16. Finally, in Fig. 17 we show the LO, NLO and NLO+NLL scale dependence for squark and gluino masses of 1 TeV and $m_{\tilde{t}_1} = 500$ GeV. The results are qualitatively very similar to those obtained for the LHC with 7 TeV, i.e. we find a strong reduction of the scale dependence when including the high-order corrections, and a very good convergence of the perturbative series at scales near $\mu = m/2$.

## 4. Conclusions

Precise theoretical predictions for sparticle cross sections are essential for the interpretation of current and future searches for supersymmetry at hadron colliders. The inclusion of higher-order SUSY-QCD corrections reduces the scale uncertainty substantially. The higher-order terms also increase the size of the cross section with respect to the LO prediction for renormalization and factorization scales near the average mass of the produced SUSY particles. Thus, the SUSY-QCD corrections have a significant impact on the extraction of SUSY mass bounds from experimental cross section limits, and would lead to a much more accurate determination of SUSY parameters like masses and couplings in the case of discovery.

In this review we have presented the state-of-the-art SUSY-QCD predictions for squark and gluino hadroproduction cross sections at the Tevatron and the LHC at 7 and 14 TeV centre-of-mass energy, including NLO corrections and NLL threshold resummation. We have discussed the impact of the SUSY-QCD corrections on the cross sections and have provided an estimate of the theoretical uncertainty due to scale variation, parton distribution functions, and the strong coupling $\alpha_s$. Special emphasis has been placed on the predictions for the LHC at 7 TeV energy, which are of immediate relevance for ongoing SUSY searches.

The effect of soft-gluon resummation is most pronounced for processes with initial-state gluons and final-state gluinos, which involve a large colour charge. Specifically, at the LHC with 7 TeV we find an increase of the cross-section prediction of up to 20% for sparticle masses around 1 TeV when going from NLO to NLO+NLL, depending in detail on the final state and the ratio of squark to gluino masses. Furthermore, the scale uncertainty is reduced significantly at NLO+NLL accuracy over the full range of sparticle masses relevant for hadron collider searches, with a remaining scale uncertainty of less than 10%. We have furthermore presented estimates for the overall theory uncertainty including the 68% C.L. pdf and $\alpha_s$ error added in quadrature, combined linearly with the scale variation error. Even though the pdf and $\alpha_s$ uncertainty is significant, the inclusion of threshold resummation leads to a sizeable reduction of the overall theory uncertainty, which is in general 20% or smaller for NLO+NLL cross sections calculated with 2008 NLO MSTW pdfs.

The NLO+NLL cross sections presented in this paper constitute the state-of-the-art QCD predictions for squark and gluino production in the MSSM, and provide therefore, we think, the optimum theoretical basis to interpret current and future searches for supersymmetry at the Tevatron and the LHC.

## Acknowledgments

This work has been supported in part by the Helmholtz Alliance “Physics at the Terascale”, the DFG Graduiertenkolleg “Elementary Particle Physics at the TeV Scale”, the Foundation for Fundamental Research of Matter (FOM) program ”Theoretical Particle Physics in the Era of the LHC”, the National Organization for Scientific Research (NWO), the DFG SFB/TR9 “Computational Particle Physics”, the European Community’s Marie-Curie Research Training Network under contract MRTN-CT-2006-035505 “Tools and Precision Calculations for Physics Discoveries at Colliders” and by the Polish Ministry of Science and Higher Education, grant MNiSW no. N202 249235.

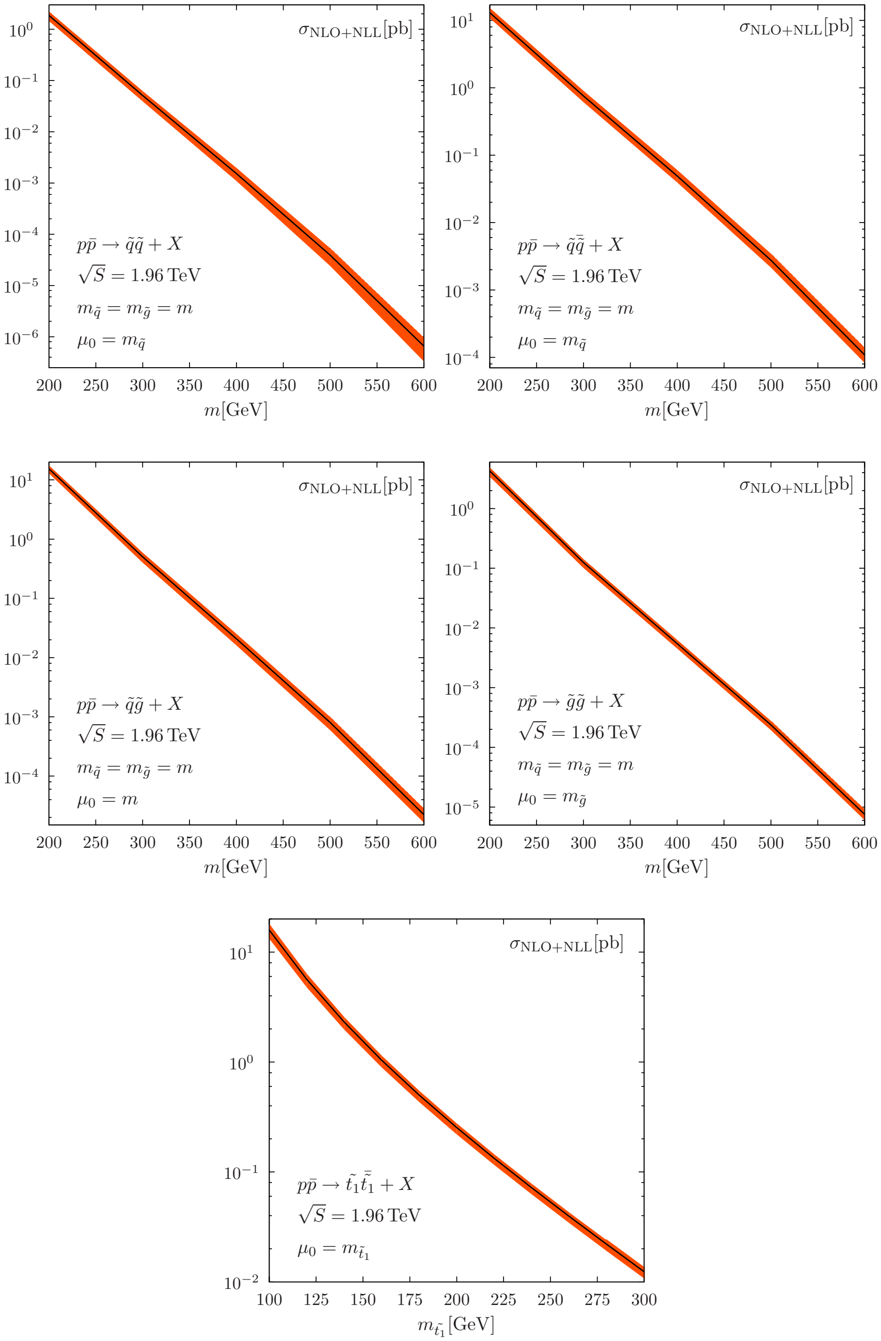

Fig. 1. The NLO+NLL SUSY-QCD cross section for the individual squark and gluino pair-production processes at the Tevatron, $p\bar{p} \to \tilde{q}\tilde{q}\,,\tilde{q}\bar{\tilde{q}}\,,\tilde{q}\tilde{g}\,,\tilde{g}\tilde{g} + X$ and $p\bar{p} \to \tilde{t}_1\bar{\tilde{t}}_1 + X$, as a function of the average sparticle mass $m$. The error band includes the 68% C.L. pdf and $\alpha_{\mathrm{s}}$ error, added in quadrature, and the error from scale variation in the range $m/2 \leq \mu \leq 2m$ added linearly to the combined pdf and $\alpha_{\mathrm{s}}$ uncertainty.

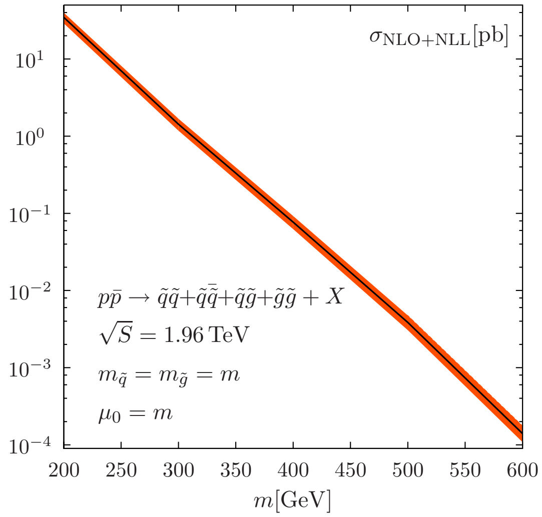

Fig. 2. The NLO+NLL SUSY-QCD cross section for inclusive squark and gluino pair-production at the Tevatron, $p\bar{p} \to \tilde{q}\tilde{q} + \tilde{q}\bar{\tilde{q}} + \tilde{q}\tilde{g} + \tilde{g}\tilde{g} + X$, as a function of the average sparticle mass $m$. The error band includes the 68% C.L. pdf and $\alpha_s$ error, added in quadrature, and the error from scale variation in the range $m/2 \leq \mu \leq 2m$ added linearly to the combined pdf and $\alpha_s$ uncertainty.

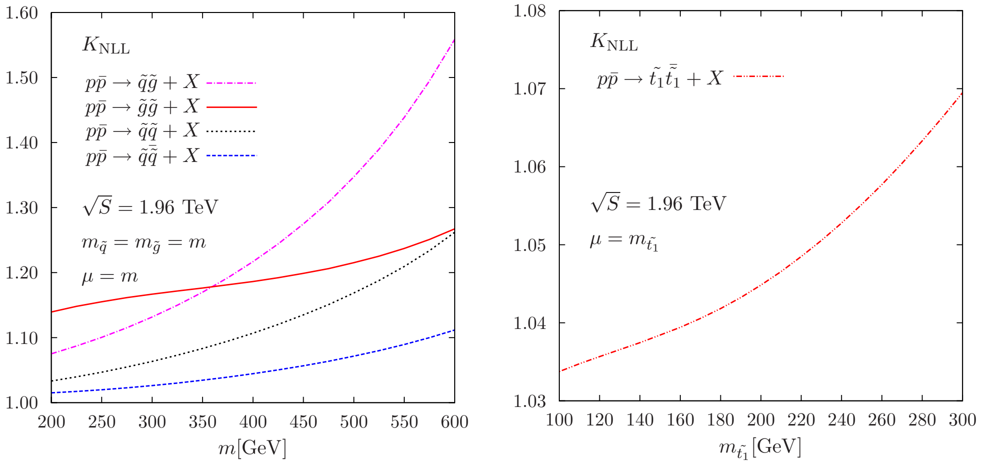

Fig. 3. The NLL $K$-factor $K_{\mathrm{NLL}} = \sigma_{\mathrm{NLO+NLL}}/\sigma_{\mathrm{NLO}}$ for the individual squark and gluino pair-production processes at the Tevatron as a function of the average sparticle mass $m$.

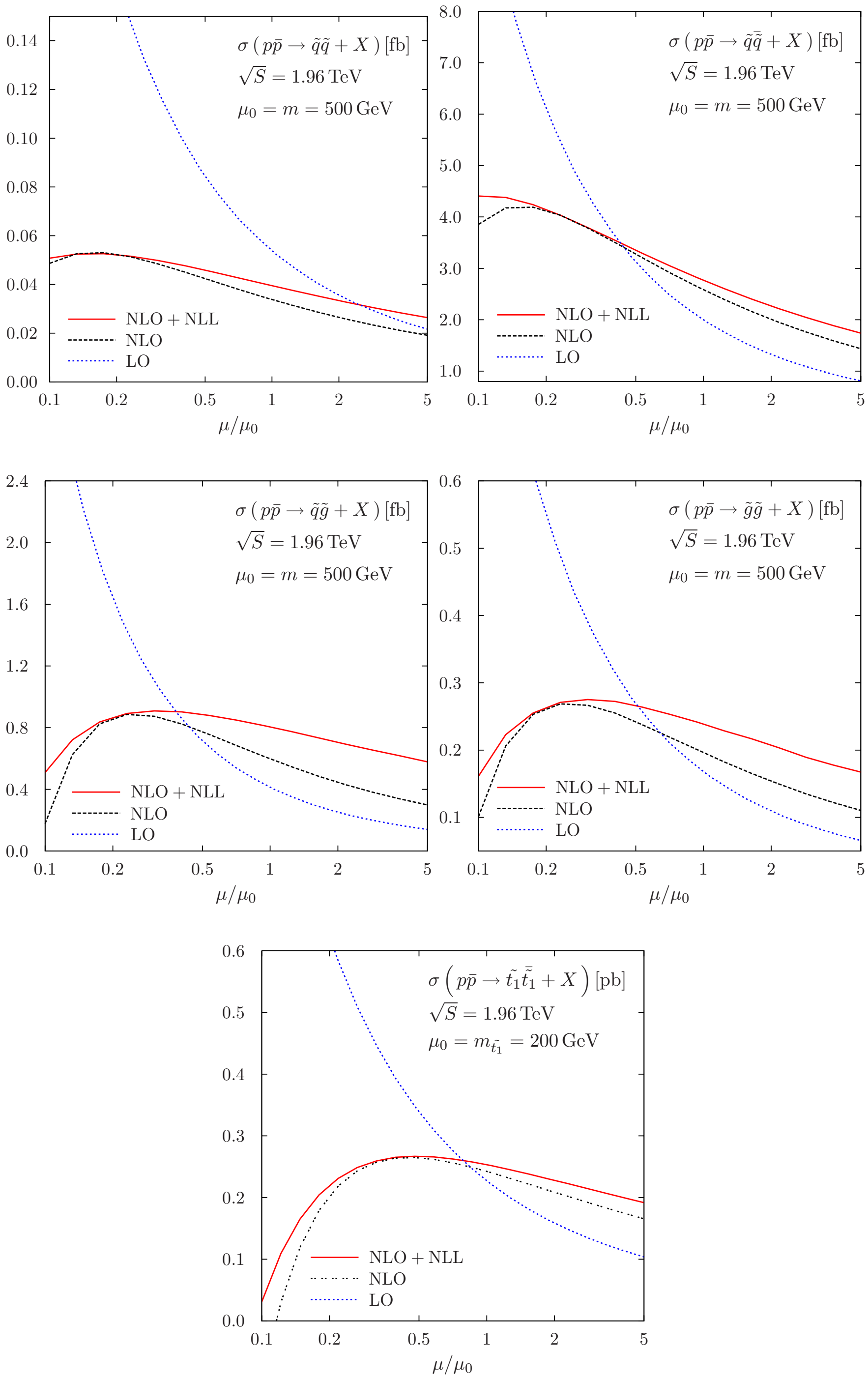

Fig. 4. The scale dependence of the LO, NLO and NLO+NLL cross sections for the individual squark and gluino pair-production processes at the Tevatron. The squark and gluino masses have been set equal $m_{\tilde{q}} = m_{\tilde{g}} = m$ in the upper four plots.

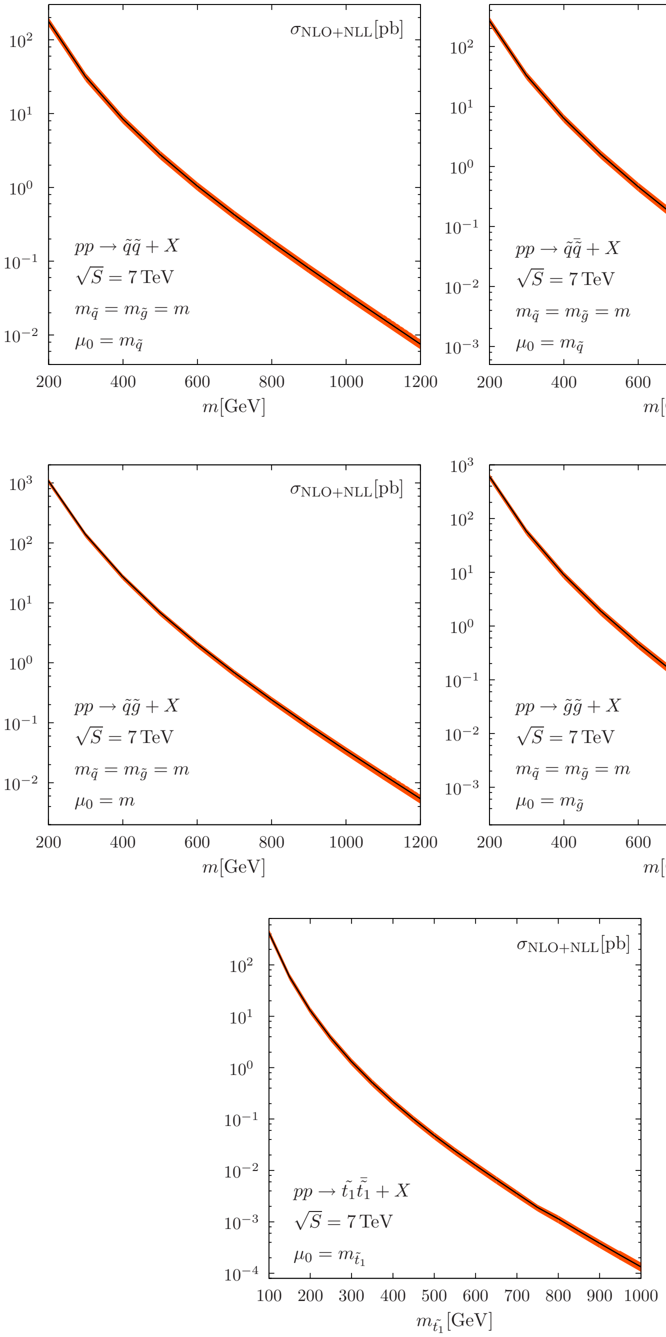

Fig. 5. The NLO+NLL SUSY-QCD cross section for the individual squark and gluino pair-production processes at the LHC with 7 TeV, $pp \to \tilde q\tilde q\,, \tilde q\bar{\tilde q}\,, \tilde q\tilde g\,, \tilde g\tilde g + X$ and $pp \to \tilde t_1\bar{\tilde t}_1 + X$, as a function of the average sparticle mass $m$. The error band includes the 68% C.L. pdf and $\alpha_{\rm s}$ error, added in quadrature, and the error from scale variation in the range $m/2 \le \mu \le 2m$ added linearly to the combined pdf and $\alpha_{\rm s}$ uncertainty.

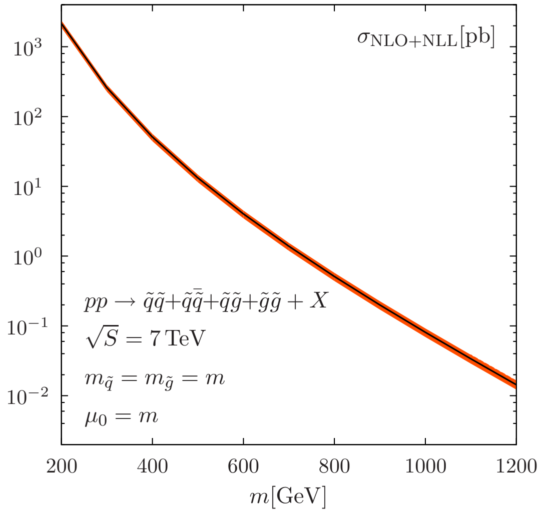

Fig. 6. The NLO+NLL SUSY-QCD cross section for inclusive squark and gluino pair-production at the LHC with 7 TeV, $pp \to \tilde{q}\tilde{q}+\tilde{q}\bar{\tilde{q}}+\tilde{q}\tilde{g}+\tilde{g}\tilde{g}+X$, as a function of the average sparticle mass $m$. The error band includes the 68% C.L. pdf and $\alpha_{\mathrm{s}}$ error, added in quadrature, and the error from scale variation in the range $m/2 \le \mu \le 2m$ added linearly to the combined pdf and $\alpha_{\mathrm{s}}$ uncertainty.

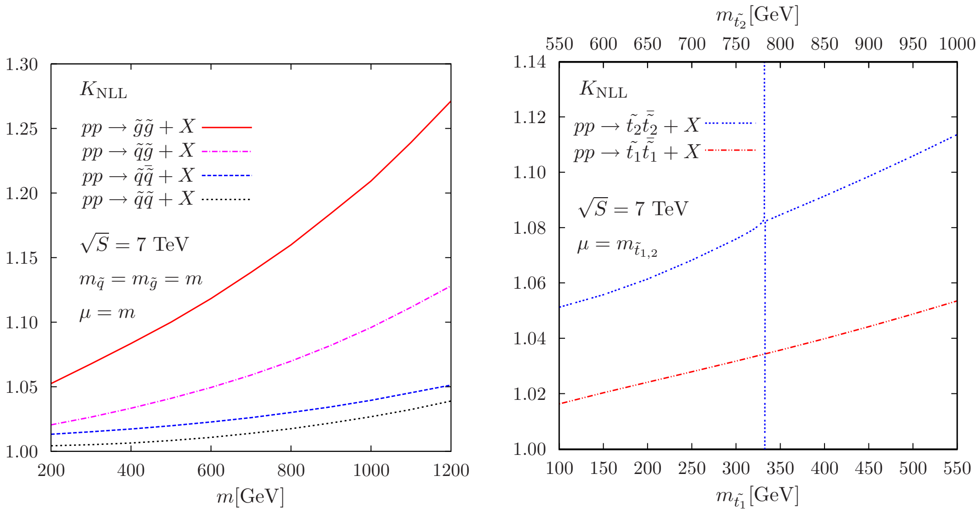

Fig. 7. The NLL $K$-factor $K_{\mathrm{NLL}} = \sigma_{\mathrm{NLO+NLL}}/\sigma_{\mathrm{NLO}}$ for the individual squark and gluino pair-production processes at the LHC with 7 TeV as a function of the average sparticle mass $m$.

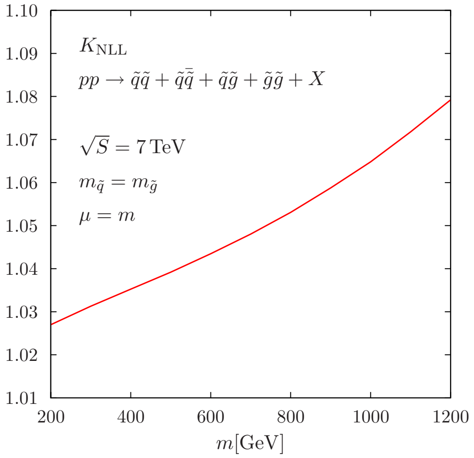

Fig. 8. The NLL $K$-factor $K_{\rm NLL} = \sigma_{\rm NLO+NLL}/\sigma_{\rm NLO}$ for for inclusive squark and gluino pair-production at the LHC with 7 TeV, $pp \to \tilde{q}\tilde{q} + \tilde{q}\bar{\tilde{q}} + \tilde{q}\tilde{g} + \tilde{g}\tilde{g} + X$, as a function of the average sparticle mass $m$.

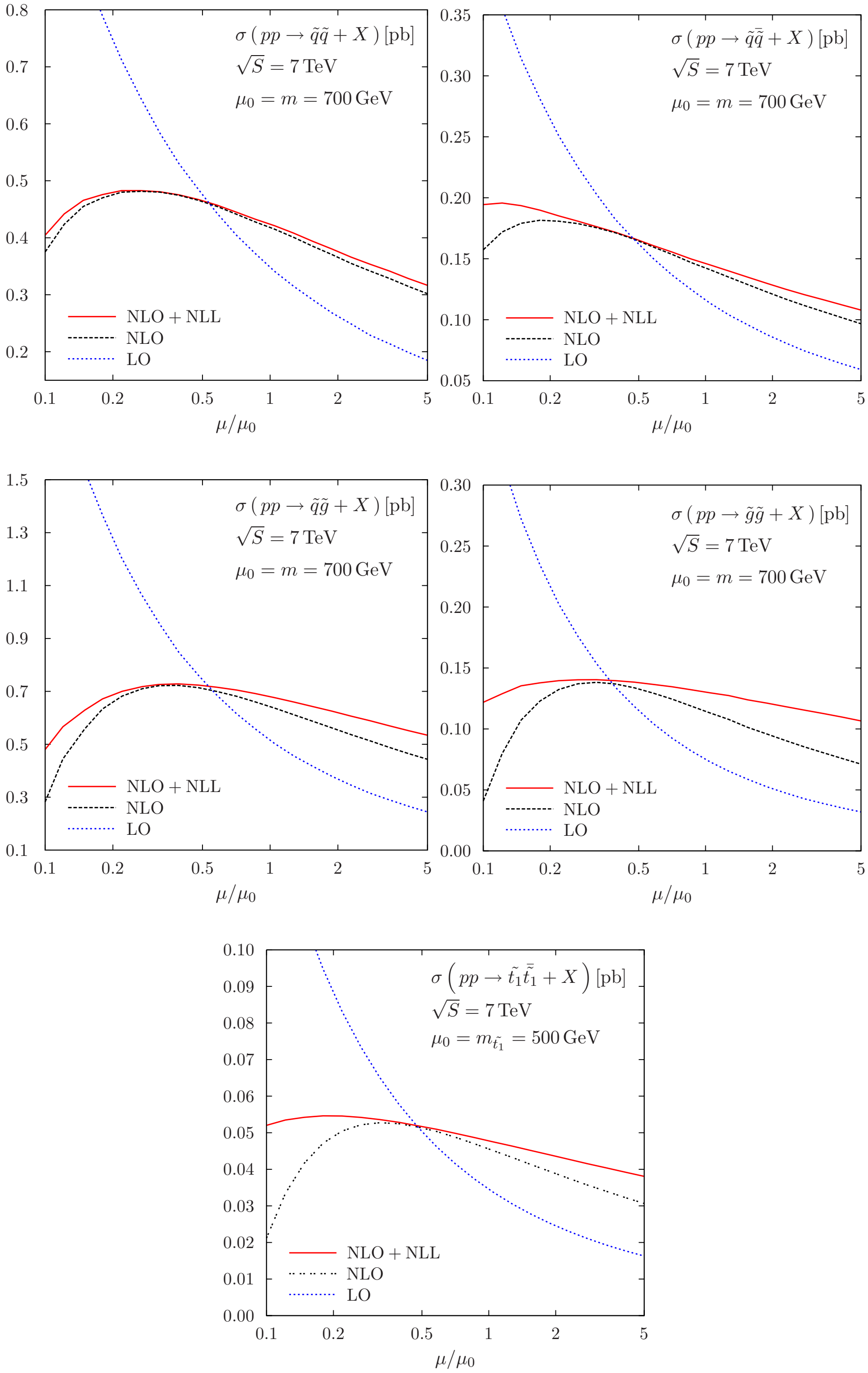

Fig. 9. The scale dependence of the LO, NLO and NLO+NLL cross sections for the individual squark and gluino pair-production processes at the LHC with 7 TeV. The squark and gluino masses have been set equal $m_{\tilde{q}} = m_{\tilde{g}} = m$ in the upper four plots.

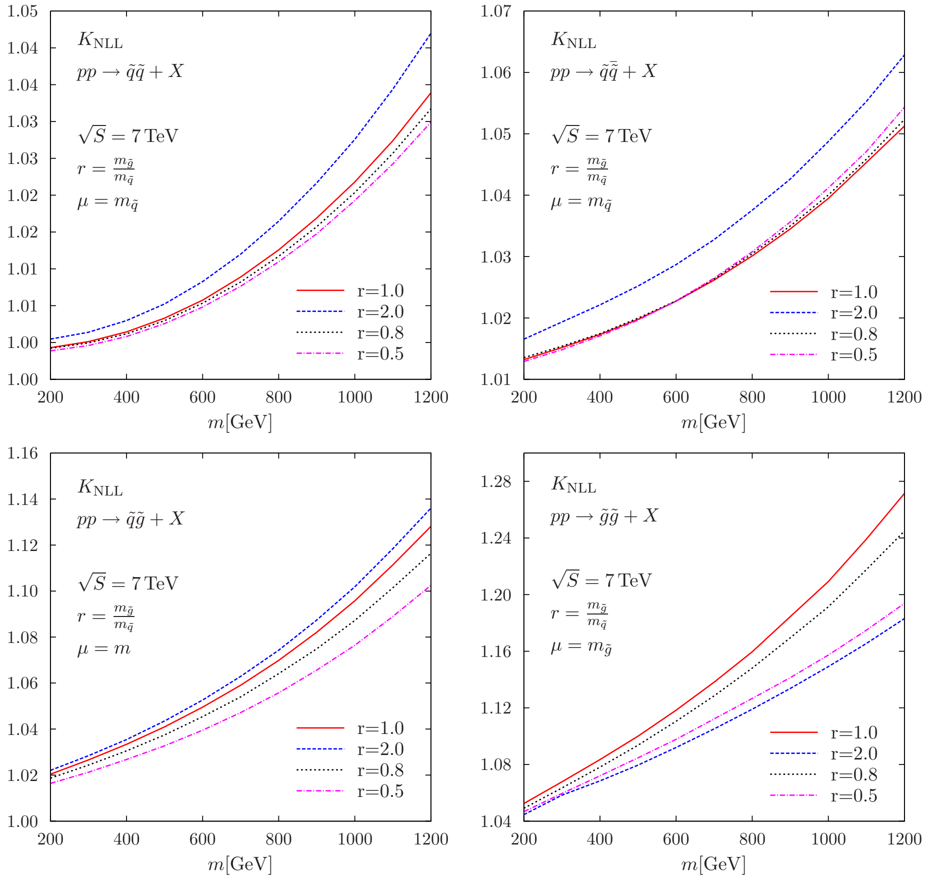

Fig. 10. The relative NLL $K$-factor $K_{\rm NLL} = \sigma_{\rm NLO+NLL}/\sigma_{\rm NLO}$ for the individual squark and gluino pair-production processes as a function of the average sparticle mass $m$, for various mass ratios $r = m_{\tilde g}/m_{\tilde q}$.

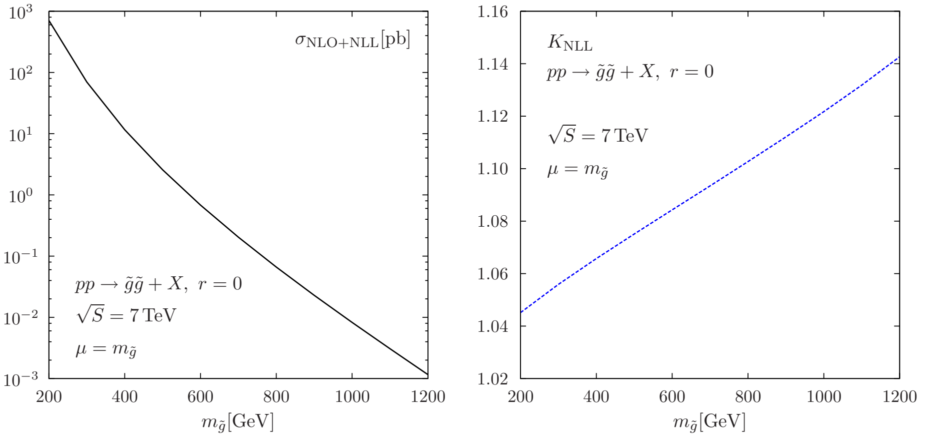

Fig. 11. The NLO+NLL SUSY-QCD cross section (left) and NLL $K$-factor (right) for gluino pair-production in the heavy squark limit, $r = m_{\tilde{g}}/m_{\tilde{q}} = 0$, at the LHC with 7 TeV, as a function of the gluino mass $m_{\tilde{g}}$.

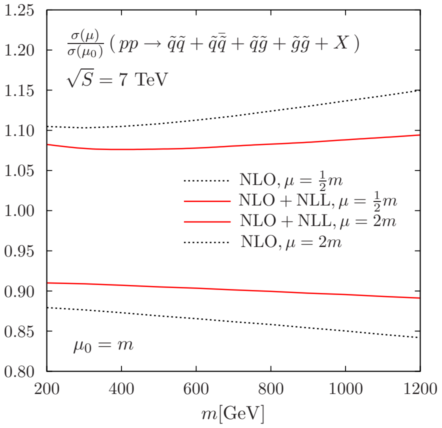

Fig. 12. The scale dependence of the NLO and NLO+NLL SUSY-QCD cross sections for inclusive squark and gluino pair-production at the LHC with 7 TeV, $pp \to \tilde{q}\tilde{q} + \tilde{q}\bar{\tilde{q}} + \tilde{q}\tilde{g} + \tilde{g}\tilde{g} + X$, as a function of the average sparticle mass $m$. Shown are results for the mass ratio $r = m_{\tilde{g}}/m_{\tilde{q}} = 1$. The upper two curves correspond to the scale set to $\mu = m/2$, the lower two curves to $\mu = 2m$.

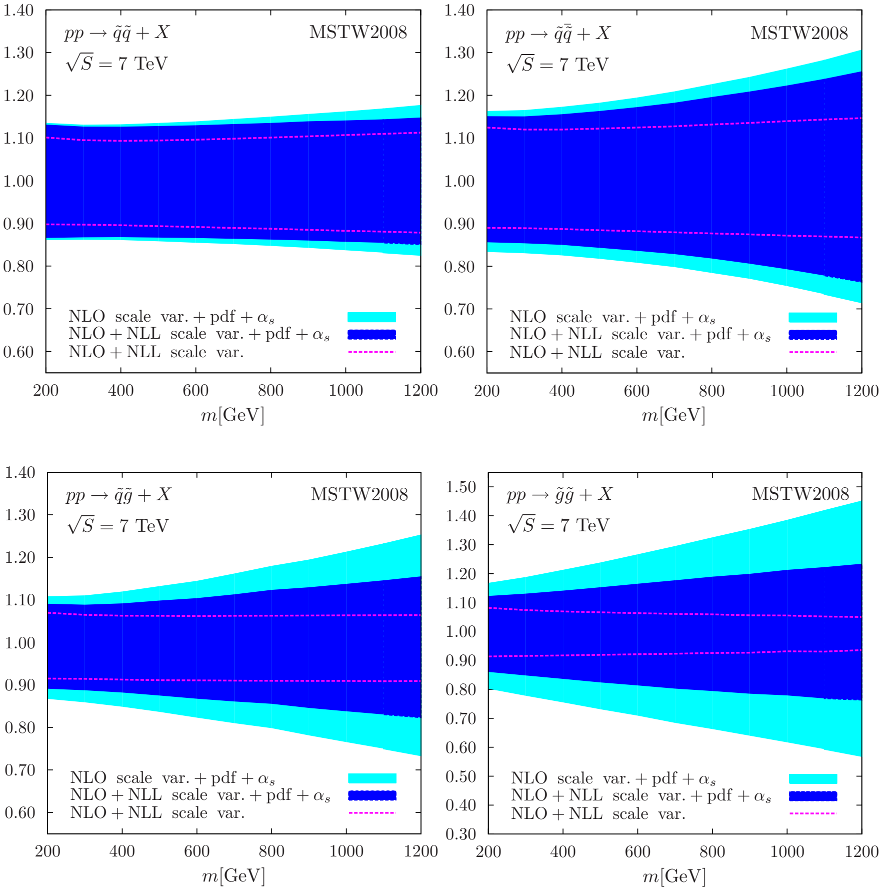

Fig. 13. The theoretical uncertainty for the the individual squark and gluino pair-production processes at the LHC with 7 TeV, $pp \to \tilde{q}\tilde{q}\,, \tilde{q}\bar{\tilde{q}}\,, \tilde{q}\tilde{g}\,, \tilde{g}\tilde{g} + X$, as a function of the sparticle mass $m_{\tilde{q}} = m_{\tilde{g}} = m$. The error bands represent the NLO+NLL scale uncertainty in the the range $m/2 \leq \mu \leq 2m$, and the total theory uncertainty including the 68% C.L. pdf and $\alpha_{\rm s}$ error, added in quadrature, and the error from scale variation in the range $m/2 \leq \mu \leq 2m$ added linearly to the combined pdf and $\alpha_{\rm s}$ uncertainty. The total theory uncertainty is shown at both NLO and NLO+NLL.

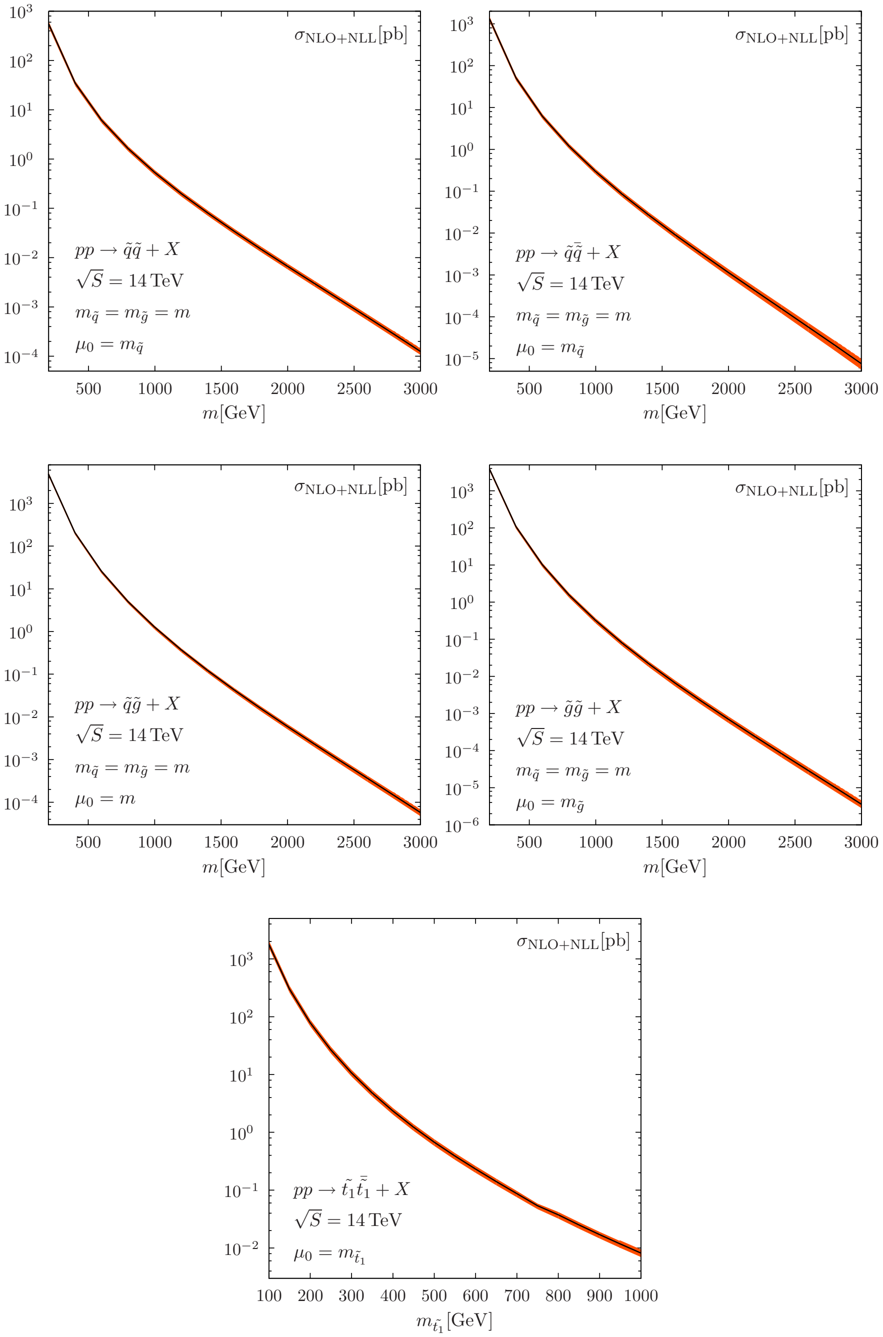

Fig. 14. The NLO+NLL SUSY-QCD cross section for the individual squark and gluino pair-production processes at the LHC with 14 TeV, $pp \to \tilde q \tilde q\,, \tilde q \bar{\tilde q}\,, \tilde q \tilde g\,, \tilde g \tilde g + X$ and $pp \to \tilde t_1 \bar{\tilde t}_1 + X$, as a function of the average sparticle mass $m$. The error band includes the 68% C.L. pdf and $\alpha_{\rm s}$ error, added in quadrature, and the error from scale variation in the range $m/2 \leq \mu \leq 2m$ added linearly to the combined pdf and $\alpha_{\rm s}$ uncertainty.

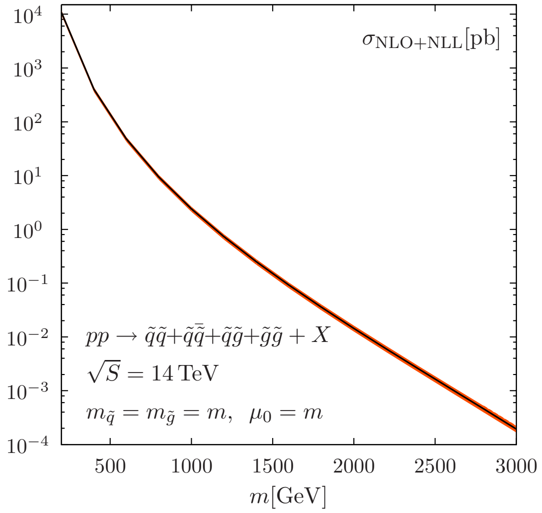

Fig. 15. The NLO+NLL SUSY-QCD cross section for inclusive squark and gluino pair-production at the LHC with 14 TeV, $pp \to \tilde{q}\tilde{q}+\tilde{q}\bar{\tilde{q}}+\tilde{q}\tilde{g}+\tilde{g}\tilde{g}+X$, as a function of the average sparticle mass $m$. The error band includes the 68% C.L. pdf and $\alpha_{\mathrm{s}}$ error, added in quadrature, and the error from scale variation in the range $m/2 \le \mu \le 2m$ added linearly to the combined pdf and $\alpha_{\mathrm{s}}$ uncertainty.

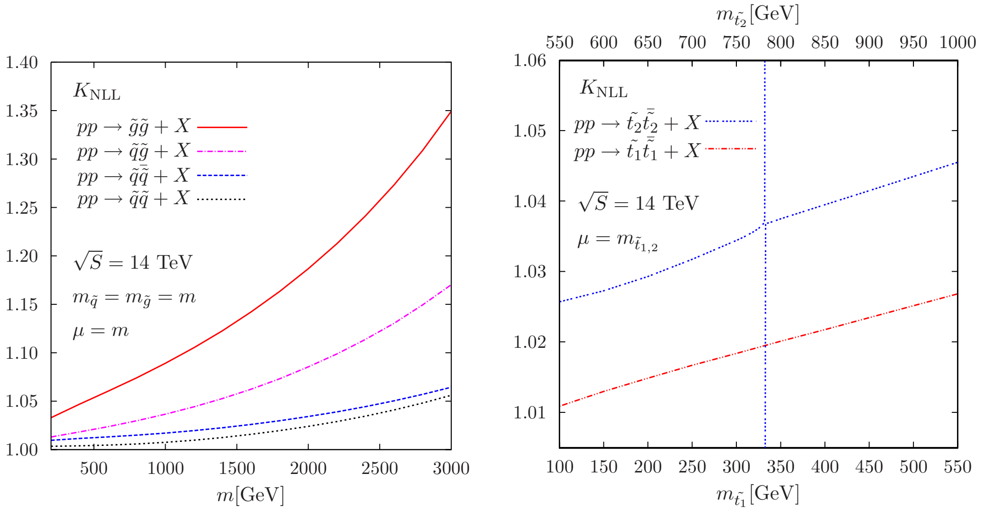

Fig. 16. The NLL $K$-factor $K_{\mathrm{NLL}} = \sigma_{\mathrm{NLO+NLL}}/\sigma_{\mathrm{NLO}}$ for the individual squark and gluino pair-production processes at the LHC with 14 TeV as a function of the average sparticle mass $m$.

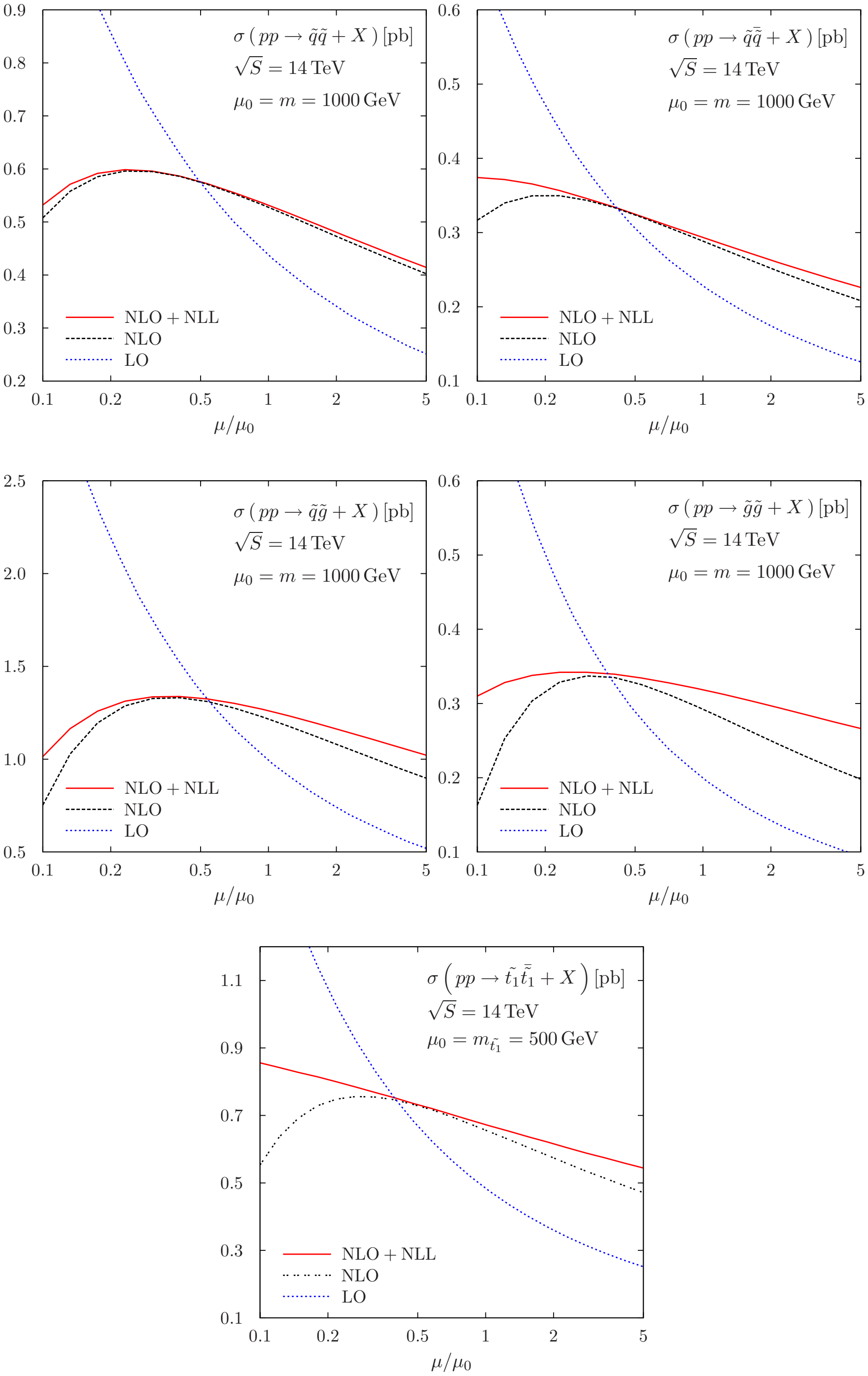

Fig. 17. The scale dependence of the LO, NLO and NLO+NLL cross sections for the individual squark and gluino pair-production processes at the LHC with 14 TeV. The squark and gluino masses have been set equal $m_{\tilde{q}} = m_{\tilde{g}} = m$ in the upper four plots.

Table 1. The LO, NLO and NLO+NLL cross sections for squark-antisquark and squark-squark production at the LHC with 7 TeV, including errors due to scale variation ($\Delta\sigma_\mu$) in the range $m_{\tilde{q}}/2 \le \mu \le 2m_{\tilde{q}}$. Results are shown for the mass ratio $r = m_{\tilde{g}}/m_{\tilde{q}} = 1$ and for two pdf parametrizations (MSTW08 and CT10) with the corresponding 68% C.L. pdf error estimates ($\Delta$pdf) and $\alpha_\mathrm{s}$-uncertainties ($\Delta\alpha_\mathrm{s}$). Note that the $\Delta$pdf and $\Delta\alpha_\mathrm{s}$ uncertainties are given as relative errors, as opposed to the absolute values of the scale variation errors.

$pp \to \tilde{q}\bar{\tilde{q}}$ at $\sqrt{S} = 7\,\mathrm{TeV}$

| | MSTW2008 | | | CT10 | | |
|---|---|---|---|---|---|---|
| $m$ [GeV] | 200 | 700 | 1200 | 200 | 700 | 1200 |
| $(\sigma \pm \Delta\sigma_\mu)_{\mathrm{LO}}$ [pb] | $195^{+68}_{-47}$ | $0.116^{+0.046}_{-0.030}$ | $\left(7.63^{+3.31}_{-2.15}\right) \times 10^{-4}$ | $165^{+54}_{-37}$ | $\left(9.63^{+3.48}_{-2.39}\right) \times 10^{-2}$ | $\left(6.09^{+2.44}_{-1.64}\right) \times 10^{-4}$ |
| $(\sigma \pm \Delta\sigma_\mu)_{\mathrm{NLO}}$ [pb] | $264^{+36}_{-35}$ | $0.143^{+0.022}_{-0.021}$ | $\left(8.31^{+1.59}_{-1.45}\right) \times 10^{-4}$ | $250^{+33}_{-32}$ | $0.141^{+0.021}_{-0.021}$ | $\left(9.65^{+1.80}_{-1.66}\right) \times 10^{-4}$ |
| $(\sigma \pm \Delta\sigma_\mu)_{\mathrm{NLO+NLL}}$ [pb] | $267^{+33}_{-30}$ | $0.146^{+0.019}_{-0.018}$ | $\left(8.73^{+1.28}_{-1.16}\right) \times 10^{-4}$ | $253^{+30}_{-27}$ | $0.144^{+0.018}_{-0.017}$ | $\left(10.11^{+1.46}_{-1.32}\right) \times 10^{-4}$ |
| $\Delta\mathrm{pdf}_{\mathrm{NLO}}$ [%] | $^{+1.5}_{-1.6}$ | $^{+5.2}_{-4.7}$ | $^{+11}_{-11}$ | $^{+2.9}_{-2.4}$ | $^{+12}_{-8}$ | $^{+37}_{-16}$ |
| $\Delta\alpha_{\mathrm{s}\,\mathrm{NLO}}$ [%] | $^{+2.4}_{-2.9}$ | $^{+2.2}_{-2.4}$ | $^{+3.6}_{-3.2}$ | $^{+2.4}_{-2.3}$ | $^{+3.1}_{-2.6}$ | $^{+5.9}_{-4.2}$ |
| $\mathrm{K}_{\mathrm{NLO}}$ | 1.35 | 1.23 | 1.09 | 1.51 | 1.46 | 1.59 |
| $\mathrm{K}_{\mathrm{NLL}}$ | 1.01 | 1.03 | 1.05 | 1.01 | 1.02 | 1.05 |

$pp \to \tilde{q}\tilde{q}$ at $\sqrt{S} = 7\,\mathrm{TeV}$

| | MSTW2008 | | | CT10 | | |
|---|---|---|---|---|---|---|
| $m$ [GeV] | 200 | 700 | 1200 | 200 | 700 | 1200 |
| $(\sigma \pm \Delta\sigma_\mu)_{\mathrm{LO}}$ [pb] | $142^{+43}_{-30}$ | $0.349^{+0.127}_{-0.087}$ | $\left(6.06^{+2.48}_{-1.65}\right) \times 10^{-3}$ | $128^{+35}_{-26}$ | $0.354^{+0.120}_{-0.084}$ | $\left(6.62^{+2.54}_{-1.72}\right) \times 10^{-3}$ |
| $(\sigma \pm \Delta\sigma_\mu)_{\mathrm{NLO}}$ [pb] | $175^{+18}_{-19}$ | $0.417^{+0.046}_{-0.051}$ | $\left(7.22^{+1.02}_{-1.06}\right) \times 10^{-3}$ | $170^{+17}_{-18}$ | $0.427^{+0.046}_{-0.052}$ | $\left(7.81^{+1.08}_{-1.13}\right) \times 10^{-3}$ |
| $(\sigma \pm \Delta\sigma_\mu)_{\mathrm{NLO+NLL}}$ [pb] | $175^{+18}_{-18}$ | $0.423^{+0.042}_{-0.047}$ | $\left(7.50^{+0.85}_{-0.91}\right) \times 10^{-3}$ | $171^{+17}_{-17}$ | $0.432^{+0.042}_{-0.047}$ | $\left(8.09^{+0.91}_{-0.99}\right) \times 10^{-3}$ |
| $\Delta\mathrm{pdf}_{\mathrm{NLO}}$ [%] | $^{+2.1}_{-1.5}$ | $^{+3.4}_{-2.4}$ | $^{+3.7}_{-2.8}$ | $^{+1.4}_{-1.4}$ | $^{+2.4}_{-2.1}$ | $^{+4.3}_{-3.5}$ |
| $\Delta\alpha_{\mathrm{s}\,\mathrm{NLO}}$ [%] | $^{+2.3}_{-2.7}$ | $^{+0.7}_{-0.9}$ | $^{+0.3}_{-0.2}$ | $^{+2.2}_{-2.2}$ | $^{+0.8}_{-0.8}$ | $^{<+0.1}_{<-0.1}$ |
| $\mathrm{K}_{\mathrm{NLO}}$ | 1.23 | 1.20 | 1.19 | 1.33 | 1.21 | 1.18 |
| $\mathrm{K}_{\mathrm{NLL}}$ | 1.00 | 1.01 | 1.04 | 1.00 | 1.01 | 1.04 |

Table 2. The LO, NLO and NLO+NLL cross sections for gluino-gluino and squark-gluino production at the LHC with 7 TeV, including errors due to scale variation ($\Delta\sigma_\mu$) in the range $m/2 \le \mu \le 2m$, where $m$ denotes the average sparticle mass. Results are shown for the mass ratio $r = m_{\tilde{g}}/m_{\tilde{q}} = 1$ and for two pdf parametrizations (MSTW08 and CT10) with the corresponding 68% C.L. pdf error estimates ($\Delta$pdf) and $\alpha_s$-uncertainties ($\Delta\alpha_s$). Note that the $\Delta$pdf and $\Delta\alpha_s$ uncertainties are given as relative errors, as opposed to the absolute values of the scale variation errors.

$pp \to \tilde{g}\tilde{g}$ at $\sqrt{S} = 7\,\mathrm{TeV}$

| | MSTW2008 | | | CT10 | | |
|---|---|---|---|---|---|---|
| $m$ [GeV] | 200 | 700 | 1200 | 200 | 700 | 1200 |
| $(\sigma \pm \Delta\sigma_\mu)_{\mathrm{LO}}$ [pb] | $420^{+184}_{-118}$ | $\left(7.51^{+3.98}_{-2.41}\right)\times10^{-2}$ | $\left(2.52^{+1.50}_{-0.87}\right)\times10^{-4}$ | $340^{+139}_{-92}$ | $\left(4.88^{+2.19}_{-1.40}\right)\times10^{-2}$ | $\left(1.48^{+0.69}_{-0.44}\right)\times10^{-4}$ |
| $(\sigma \pm \Delta\sigma_\mu)_{\mathrm{NLO}}$ [pb] | $576^{+72}_{-81}$ | $0.114^{+0.019}_{-0.020}$ | $\left(4.12^{+0.91}_{-0.88}\right)\times10^{-4}$ | $541^{+65}_{-74}$ | $0.123^{+0.019}_{-0.021}$ | $\left(5.72^{+1.25}_{-1.23}\right)\times10^{-4}$ |
| $(\sigma \pm \Delta\sigma_\mu)_{\mathrm{NLO+NLL}}$ [pb] | $606^{+49}_{-52}$ | $0.130^{+0.008}_{-0.010}$ | $\left(5.25^{+0.26}_{-0.34}\right)\times10^{-4}$ | $569^{+44}_{-46}$ | $0.138^{+0.008}_{-0.011}$ | $\left(7.08^{+0.43}_{-0.55}\right)\times10^{-4}$ |
| $\Delta\mathrm{pdf}_{\mathrm{NLO}}$ [%] | $^{+3.8}_{-4.7}$ | $^{+12}_{-13}$ | $^{+22}_{-21}$ | $^{+6.4}_{-5.4}$ | $^{+30}_{-18}$ | $^{+87}_{-35}$ |
| $\Delta\alpha_{s\,\mathrm{NLO}}$ [%] | $^{+2.3}_{-2.8}$ | $^{+4.4}_{-4.6}$ | $^{+7.6}_{-6.9}$ | $^{+2.6}_{-2.4}$ | $^{+6.1}_{-4.9}$ | $^{+13}_{-9}$ |
| $\mathrm{K}_{\mathrm{NLO}}$ | 1.37 | 1.52 | 1.64 | 1.59 | 2.52 | 3.86 |
| $\mathrm{K}_{\mathrm{NLL}}$ | 1.05 | 1.14 | 1.27 | 1.05 | 1.13 | 1.24 |

$pp \to \tilde{q}\tilde{g}$ at $\sqrt{S} = 7\,\mathrm{TeV}$

| | MSTW2008 | | | CT10 | | |
|---|---|---|---|---|---|---|
| $m$ [GeV] | 200 | 700 | 1200 | 200 | 700 | 1200 |
| $(\sigma \pm \Delta\sigma_\mu)_{\mathrm{LO}}$ [pb] | $917^{+330}_{-225}$ | $0.515^{+0.228}_{-0.147}$ | $\left(3.66^{+1.84}_{-1.14}\right)\times10^{-3}$ | $824^{+280}_{-194}$ | $0.434^{+0.174}_{-0.116}$ | $\left(2.93^{+1.27}_{-0.83}\right)\times10^{-3}$ |
| $(\sigma \pm \Delta\sigma_\mu)_{\mathrm{NLO}}$ [pb] | $\left(1.07^{+0.09}_{-0.12}\right)\times10^{3}$ | $0.642^{+0.069}_{-0.088}$ | $\left(4.81^{+0.73}_{-0.81}\right)\times10^{-3}$ | $\left(1.02^{+0.08}_{-0.11}\right)\times10^{3}$ | $0.657^{+0.068}_{-0.088}$ | $\left(5.74^{+0.84}_{-0.96}\right)\times10^{-3}$ |
| $(\sigma \pm \Delta\sigma_\mu)_{\mathrm{NLO+NLL}}$ [pb] | $\left(1.09^{+0.07}_{-0.09}\right)\times10^{3}$ | $0.680^{+0.042}_{-0.061}$ | $\left(5.43^{+0.35}_{-0.49}\right)\times10^{-3}$ | $\left(1.04^{+0.07}_{-0.09}\right)\times10^{3}$ | $0.693^{+0.042}_{-0.061}$ | $\left(6.39^{+0.43}_{-0.61}\right)\times10^{-3}$ |
| $\Delta\mathrm{pdf}_{\mathrm{NLO}}$ [%] | $^{+0.9}_{-1.0}$ | $^{+4.7}_{-4.9}$ | $^{+9.7}_{-9.3}$ | $^{+1.8}_{-1.5}$ | $^{+11}_{-8}$ | $^{+32}_{-16}$ |
| $\Delta\alpha_{s\,\mathrm{NLO}}$ [%] | $^{+1.8}_{-2.3}$ | $^{+2.0}_{-2.3}$ | $^{+3.1}_{-3.0}$ | $^{+1.9}_{-1.8}$ | $^{+2.6}_{-2.2}$ | $^{+5.1}_{-4.1}$ |
| $\mathrm{K}_{\mathrm{NLO}}$ | 1.16 | 1.25 | 1.32 | 1.24 | 1.52 | 1.96 |
| $\mathrm{K}_{\mathrm{NLL}}$ | 1.02 | 1.06 | 1.13 | 1.02 | 1.06 | 1.11 |

Table 3. The LO, NLO and NLO+NLL cross sections for stop-antistop production at the LHC with 7 TeV, including errors due to scale variation ($\Delta\sigma_\mu$) in the range $m_{\tilde{t}}/2 \le \mu \le 2m_{\tilde{t}}$. The SUSY parameters $m_{\tilde{g}}$, $m_{\tilde{q}}$ and $\theta_{\tilde{t}}$ have been set to the SPS1a' benchmark values. Results are shown for two pdf parametrizations (MSTW08 and CT10) with the corresponding 68% C.L. pdf error estimates ($\Delta$pdf) and $\alpha_s$-uncertainties ($\Delta\alpha_s$). Note that the $\Delta$pdf and $\Delta\alpha_s$ uncertainties are given as relative errors, as opposed to the absolute values of the scale variation errors.

$$pp \to \tilde{t}_1\bar{\tilde{t}}_1 \text{ at } \sqrt{S} = 7\,\text{TeV}$$

| | MSTW2008 | | CT10 | |
|---|---|---|---|---|
| $m_{\tilde{t}_1}$ [GeV] | 100 | 400 | 100 | 400 |
| $(\sigma \pm \Delta\sigma_\mu)_{\rm LO}$ [pb] | $305^{+114}_{-77}$ | $0.156^{+0.070}_{-0.044}$ | $265^{+95}_{-65}$ | $0.119^{+0.048}_{-0.032}$ |
| $(\sigma \pm \Delta\sigma_\mu)_{\rm NLO}$ [pb] | $416^{+64}_{-59}$ | $0.209^{+0.027}_{-0.031}$ | $389^{+58}_{-53}$ | $0.202^{+0.025}_{-0.029}$ |
| $(\sigma \pm \Delta\sigma_\mu)_{\rm NLO+NLL}$ [pb] | $423^{+60}_{-46}$ | $0.218^{+0.020}_{-0.020}$ | $395^{+54}_{-42}$ | $0.209^{+0.018}_{-0.019}$ |
| $\Delta\text{pdf}_{\rm NLO}$ [%] | $^{+2.0}_{-2.4}$ | $^{+5.8}_{-6.3}$ | $^{+2.7}_{-2.5}$ | $^{+11}_{-9}$ |
| $\Delta\alpha_{\rm s NLO}$ [%] | $^{+2.1}_{-2.5}$ | $^{+2.7}_{-3.1}$ | $^{+2.1}_{-2.1}$ | $^{+3.2}_{-2.8}$ |
| $\rm K_{NLO}$ | 1.37 | 1.34 | 1.47 | 1.70 |
| $\rm K_{NLL}$ | 1.02 | 1.04 | 1.02 | 1.04 |

$$pp \to \tilde{t}_2\bar{\tilde{t}}_2 \text{ at } \sqrt{S} = 7\,\text{TeV}$$

| | MSTW2008 | | CT10 | |
|---|---|---|---|---|
| $m_{\tilde{t}_2}$ [GeV] | 600 | 1000 | 600 | 1000 |
| $(\sigma \pm \Delta\sigma_\mu)_{\rm LO}$ [pb] | $(9.06^{+4.22}_{-2.66}) \times 10^{-3}$ | $(9.64^{+4.83}_{-2.97}) \times 10^{-5}$ | $(6.63^{+2.70}_{-1.78}) \times 10^{-3}$ | $(6.76^{+2.86}_{-1.88}) \times 10^{-5}$ |
| $(\sigma \pm \Delta\sigma_\mu)_{\rm NLO}$ [pb] | $(1.23^{+0.18}_{-0.20}) \times 10^{-2}$ | $(1.17^{+0.15}_{-0.19}) \times 10^{-4}$ | $(1.24^{+0.18}_{-0.20}) \times 10^{-2}$ | $(1.33^{+0.17}_{-0.22}) \times 10^{-4}$ |
| $(\sigma \pm \Delta\sigma_\mu)_{\rm NLO+NLL}$ [pb] | $(1.30^{+0.13}_{-0.12}) \times 10^{-2}$ | $(1.31^{+0.05}_{-0.09}) \times 10^{-4}$ | $(1.30^{+0.12}_{-0.13}) \times 10^{-2}$ | $(1.47^{+0.06}_{-0.11}) \times 10^{-4}$ |
| $\Delta\text{pdf}_{\rm NLO}$ [%] | $^{+8.3}_{-8.7}$ | $^{+14}_{-13}$ | $^{+18}_{-12}$ | $^{+42}_{-20}$ |
| $\Delta\alpha_{\rm s NLO}$ [%] | $^{+3.2}_{-3.5}$ | $^{+4.3}_{-4.0}$ | $^{+4.2}_{-3.5}$ | $^{+7.0}_{-5.4}$ |
| $\rm K_{NLO}$ | 1.36 | 1.22 | 1.87 | 1.97 |
| $\rm K_{NLL}$ | 1.06 | 1.11 | 1.05 | 1.10 |

## References

1. Yu. A. Golfand and E. P. Likhtman, *JETP Lett.* **13**, 323 (1971) [Pisma Zh. Eksp. Teor. Fiz. **13**, 452 (1971)].
2. J. Wess and B. Zumino, *Nucl. Phys. B* **70**, 39 (1974).
3. H. P. Nilles, *Phys. Rept.* **110**, 1 (1984).
4. H. E. Haber and G. L. Kane, *Phys. Rept.* **117**, 75 (1985).
5. J. R. Ellis and S. Rudaz, *Phys. Lett. B* **128**, 248 (1983).
6. D0 Collaboration (V. M. Abazov *et al.*), *Phys. Lett. B* **660**, 449 (2008) [arXiv:0712.3805 [hep-ex]].
7. CDF Collaboration (T. Aaltonen *et al.*), *Phys. Rev. Lett.* **102**, 121801 (2009) [arXiv:0811.2512 [hep-ex]].
8. V. Khachatryan *et al.* [CMS Collaboration], Phys. Lett. **B698** (2011) 196-218. [arXiv:1101.1628 [hep-ex]].
9. G. Aad *et al.* [Atlas Collaboration], [arXiv:1102.2357 [hep-ex]].
10. G. Aad *et al.* [Atlas Collaboration], [arXiv:1102.5290 [hep-ex]].
11. S. Chatrchyan *et al.* [CMS Collaboration], [arXiv:1103.0953 [hep-ex]].
12. S. Chatrchyan *et al.* [CMS Collaboration], [arXiv:1103.1348 [hep-ex]].
13. G. Aad *et al.* [ATLAS Collaboration], [arXiv:1103.4344 [hep-ex]].
14. LEPSUSYWG, ALEPH, DELPHI, L3, and OPAL experiments, note LEPSUSYWG/04-02.1 (http://lepsusy.web.cern.ch/lepsusy/Welcome.html).
15. ALEPH Collaboration (A. Heister *et al.*), *Phys. Lett. B* **537**, 5 (2002) [arXiv:hep-ex/0204036].
16. CDF Collaboration (T. Aaltonen *et al.*), *Phys. Rev. D* **76**, 072010 (2007) [arXiv:0707.2567 [hep-ex]].
17. D0 Collaboration (V.M. Abazov *et al.*), *Phys. Lett. B* **665**, 1 (2008) [arXiv:0803.2263 [hep-ex]].
18. D0 Collaboration (V. M. Abazov *et al.*), *Phys. Lett. B* **675**, 289 (2009) [arXiv:0811.0459 [hep-ex]].
19. P. Bechtle, K. Desch, H. K. Dreiner, M. Krämer, B. O'Leary, C. Robens, B. Sarrazin, P. Wienemann, [arXiv:1102.4693 [hep-ph]].
20. The ATLAS Collaboration (G. Aad *et al.*), arXiv:0901.0512 [hep-ex].
21. CMS Collaboration (G. L. Bayatian *et al.*), *J. Phys. G* **34**, 995 (2007).
22. see e.g. H. Baer, V. Barger, G. Shaughnessy, H. Summy and L. t. Wang, *Phys. Rev. D* **75**, 095010 (2007) [arXiv:hep-ph/0703289].
23. G. L. Kane, A. A. Petrov, J. Shao and L. T. Wang, *J. Phys. G* **37**, 045004 (2010) [arXiv:0805.1397 [hep-ph]].
24. J. Hubisz, J. Lykken, M. Pierini, M. Spiropulu, Phys. Rev. **D78** (2008) 075008. [arXiv:0805.2398 [hep-ph]].
25. H. K. Dreiner, M. Krämer, J. M. Lindert, B. O'Leary, JHEP **1004** (2010) 109. [arXiv:1003.2648 [hep-ph]].
26. G. L. Kane and J. P. Leveille, *Phys. Lett. B* **112**, 227 (1982).
27. P. R. Harrison and C. H. Llewellyn Smith, *Nucl. Phys. B* **213**, 223 (1983) [*Erratum-ibid. B* **223**, 542 (1983)].
28. S. Dawson, E. Eichten and C. Quigg, *Phys. Rev. D* **31**, 1581 (1985).
29. W. Beenakker, R. Höpker, M. Spira and P. M. Zerwas, *Phys. Rev. Lett.* **74**, 2905 (1995) [arXiv:hep-ph/9412272].
30. W. Beenakker, R. Höpker, M. Spira and P. M. Zerwas, *Z. Phys. C* **69**, 163 (1995) [arXiv:hep-ph/9505416].
31. W. Beenakker, R. Höpker, M. Spira and P. M. Zerwas, *Nucl. Phys. B* **492**, 51 (1997) [arXiv:hep-ph/9610490].

32. W. Beenakker, M. Krämer, T. Plehn, M. Spira and P. M. Zerwas, *Nucl. Phys. B* **515**, 3 (1998) [arXiv:hep-ph/9710451].
33. W. Hollik, M. Kollar and M. K. Trenkel, *JHEP* **0802**, 018 (2008) [arXiv:0712.0287 [hep-ph]].
34. W. Hollik and E. Mirabella, *JHEP* **0812**, 087 (2008) [arXiv:0806.1433 [hep-ph]].
35. W. Hollik, E. Mirabella and M. K. Trenkel, *JHEP* **0902**, 002 (2009) [arXiv:0810.1044 [hep-ph]].
36. M. Beccaria, G. Macorini, L. Panizzi, F. M. Renard and C. Verzegnassi, *Int. J. Mod. Phys. A* **23**, 4779 (2008) [arXiv:0804.1252 [hep-ph]].
37. E. Mirabella, *JHEP* **0912**, 012 (2009) [arXiv:0908.3318 [hep-ph]].
38. J. Germer, W. Hollik, E. Mirabella, M. K. Trenkel, JHEP **1008** (2010) 023. [arXiv:1004.2621 [hep-ph]].
39. J. Germer, W. Hollik, E. Mirabella, [arXiv:1103.1258 [hep-ph]].
40. A. T. Alan, K. Cankocak and D. A. Demir, *Phys. Rev. D* **75**, 095002 (2007) [*Erratum-ibid. D* **76**, 119903 (2007)] [arXiv:hep-ph/0702289].
41. S. Bornhauser, M. Drees, H. K. Dreiner and J. S. Kim, *Phys. Rev. D* **76**, 095020 (2007) [arXiv:0709.2544 [hep-ph]].
42. G. F. Sterman, Nucl. Phys. B **281** (1987) 310.
43. S. Catani and L. Trentadue, Nucl. Phys. B **327** (1989) 323.
44. A. Kulesza and L. Motyka, *Phys. Rev. Lett.* **102**, 111802 (2009) [arXiv:0807.2405 [hep-ph]].
45. A. Kulesza and L. Motyka, *Phys. Rev. D* **80**, 095004 (2009) [arXiv:0905.4749 [hep-ph]].
46. W. Beenakker, S. Brensing, M. Krämer, A. Kulesza, E. Laenen and I. Niessen, *JHEP* **0912**, 041 (2009) [arXiv:0909.4418 [hep-ph]].
47. W. Beenakker, S. Brensing, M. Krämer, A. Kulesza, E. Laenen and I. Niessen, *JHEP* **1008**, 098 (2010) [arXiv:1006.4771 [hep-ph]].
48. M. Beneke, P. Falgari and C. Schwinn, *Nucl. Phys. B* **828**, 69 (2010) [arXiv:0907.1443 [hep-ph]].
49. M. Beneke, P. Falgari, C. Schwinn, Nucl. Phys. **B842**, 414-474 (2011). [arXiv:1007.5414 [hep-ph]].
50. U. Langenfeld and S. O. Moch, *Phys. Lett. B* **675**, 210 (2009) [arXiv:0901.0802 [hep-ph]].
51. U. Langenfeld, [arXiv:1011.3341 [hep-ph]].
52. K. Hagiwara and H. Yokoya, *JHEP* **0910**, 049 (2009) [arXiv:0909.3204 [hep-ph]].
53. M. R. Kauth, J. H. Kuhn, P. Marquard, M. Steinhauser, Nucl. Phys. **B831** (2010) 285-305 [arXiv:0910.2612 [hep-ph]].
54. N. Kidonakis and G. F. Sterman, Nucl. Phys. B **505** (1997) 321 [arXiv:hep-ph/9705234].
55. R. Bonciani, S. Catani, M. L. Mangano and P. Nason, Nucl. Phys. B **529** (1998) 424 [Erratum-ibid. B **803** (2008) 234] [arXiv:hep-ph/9801375].
56. N. Kidonakis, G. Oderda and G. F. Sterman, Nucl. Phys. B **525** (1998) 299 [arXiv:hep-ph/9801268].
57. N. Kidonakis, G. Oderda and G. F. Sterman, Nucl. Phys. B **531** (1998) 365 [arXiv:hep-ph/9803241].
58. R. Bonciani, S. Catani, M. L. Mangano and P. Nason, Phys. Lett. B **575**, (2003) 268 [arXiv:hep-ph/0307035].
59. S. Catani, M. L. Mangano, P. Nason and L. Trentadue, Nucl. Phys. B **478** (1996) 273 [arXiv:hep-ph/9604351].
60. see `http://www.thphys.uni-heidelberg.de/~plehn/prospino/` or `http://people.web.psi.ch/spira/prospino/`

61. J. A. Aguilar-Saavedra *et al.*, Eur. Phys. J. C **46** (2006) 43 [arXiv:hep-ph/0511344].
62. MSTW, private communication: parton distribution functions with improved accuracy in the evolution at large $x$, based on the MSTW parametrization at the input scale.[63]
63. A. D. Martin, W. J. Stirling, R. S. Thorne and G. Watt, Eur. Phys. J. C **63** (2009) 189 [arXiv:0901.0002 [hep-ph]].
64. H. L. Lai, M. Guzzi, J. Huston, Z. Li, P. M. Nadolsky, J. Pumplin and C. P. Yuan, Phys. Rev. D **82** (2010) 074024 [arXiv:1007.2241 [hep-ph]].
65. J. Pumplin, D.R. Stump, J. Huston, H.L. Lai, P. Nadolsky, W.K. Tung, JHEP 0207:012(2002) [arXiv: hep-ph/0201195].
66. M. Botje, J. Butterworth, A. Cooper-Sarkar, A. de Roeck, J. Feltesse, S. Forte, A. Glazov, J. Huston *et al.*, [arXiv:1101.0538 [hep-ph]].
67. N. Arkani-Hamed and S. Dimopoulos, JHEP **0506** (2005) 073 [arXiv:hep-th/0405159].
68. V. Khachatryan *et al.* [CMS Collaboration], Phys. Rev. Lett. **106** (2011) 011801 [arXiv:1011.5861 [hep-ex]].
69. G. Aad *et al.* [ ATLAS Collaboration ], [arXiv:1103.1984 [hep-ex]].